Gold Nanostructures

DOI: 10.1002/anie.200804634

Facile Synthesis of Branched Au Nanostructures by Templating Against a Self-Destructive Lattice of Magnetic Fe Nanoparticles**

*Zhengquan Li, Weiyang Li, Pedro H. C. Camargo, and Younan Xia**

Controlling the shape or morphology of metal nanostructures has attracted considerable attention, as it provides an effective means for tuning the electronic, optical, magnetic, and catalytic properties.[1] In particular, synthesis of Au nanostructures with controllable shapes has become the aim of extensive research over the past decade, owing to their unique optical properties known as localized surface plasmon resonance (LSPR).[2] Most of the published work, however, has focused on the synthesis of simple Au nanostructures, such as spheres, cubes, plates, and rods, among others.[3] Only in recent years, have reports on the chemical syntheses of complex, branched Au nanostructures arisen.[4,5] Gold nanostructures with a branched morphology could be useful in areas such as catalysis, sensing, and flexible electronics. Calculations by discrete dipole approximation (DDA) and finite-difference time domain (FDTD) methods have revealed that the tips of a branched Au nanostructure can exhibit strong enhancement of an electromagnetic field, which is of great importance to applications such as surface-enhanced Raman scattering (SERS).[5] However, unlike semiconductor nanocrystals, in which the branched, anisotropic growth can be naturally induced by polymorphism (for example, switching between zinc blende and wurtzite structures),[6] formation of branched nanostructures from a face-centered cubic (fcc) metal has proven to be difficult and very sensitive to experimental conditions. Although branched[4,5] and star-shaped[7] Au nanoparticles have been obtained through the growth of Au nanocrystallite seeds, in most cases the cores are large and the branching tips are relatively short. To our knowledge, it remains a challenge to develop a rational and effective method for preparing highly branched Au nanostructures in high yields.

Template-directed synthesis, a straightforward route to nanostructures with predefined shapes, has been widely used to generate inorganic nanostructures in high yields.[8] In general, the template serves as a scaffold, within (or around) which a different material is produced and shaped into a nanostructure with its shape or morphology complementary to that of the template. Owing to limitations imposed by the availability of templates, this approach has mainly been applied to the preparation of nanostructures in a zero- or one-dimensional morphology. In many cases, the templates have to be removed by etching or calcination to isolate the final products. This last step is generally slow and difficult, owing to diffusion problems, and may cause damage to the desired nanostructures. Herein, we demonstrate a reactive and self-destructive template that not only participates in the chemical reaction but also spontaneously falls apart at a certain point to release the products. The template is a three-dimensional porous lattice consisting of uniform Fe nanoparticles self-assembled on a magnetic stirrer bar.[9] On addition of AuCl, a galvanic replacement reaction takes place between Fe and Au^+, leading to the formation of highly branched Au nanostructures in the void space of the lattice.[10] As the Fe nanoparticles are reduced in size by the replacement reaction, their magnetic moments are also reduced accordingly, and eventually the lattice falls apart to release the Au nanostructures. This approach is somewhat similar to those reported in previous studies that used the voids in crystalline lattices of latex spheres to produce inverse opals[11] or large anisotropic colloidal particles.[12] However, there are a number of major differences that should highlighted: a) the current system works on a scale almost 100-times smaller than those based on latex spheres; b) the template itself is also directly involved in the reaction; c) the template spontaneously disassembles during the synthesis; and d) the final product has a highly branched morphology.

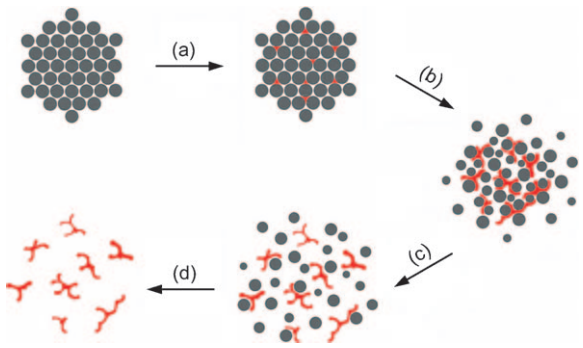

Figure 1. The four major steps involved in the formation of Au multipods by templating against a self-destructive lattice of Fe nanoparticles: a) Au nucleates in the voids of aggregated Fe nanoparticles through a replacement reaction between Fe and Au^+; b) Au evolves into multipods under the confinement of Fe nanoparticles as the reaction proceeds; c) the lattice of Fe nanoparticles falls apart as the volume of Au structures increases and the magnetic moments of individual Fe nanoparticles are reduced; and d) Au multipods are harvested and purified by dissolving the remaining Fe nanoparticles with H_2SO_4.

[*] Dr. Z. Li, W. Li, P. H. C. Camargo, Prof. Y. Xia
Department of Biomedical Engineering, Washington University
Saint Louis, MO 63130 (USA)
E-mail: xia@biomed.wustl.edu

[**] This work was supported in part by research grants from the NSF (DMR, 0451788 and 0804088) and a Director's Pioneer Award from the NIH (5DP1OD000798). P.H.C.C. was supported in part by the Fulbright Program and the Brazilian Ministry of Education (CAPES).

Supporting information for this article is available on the WWW under http://dx.doi.org/10.1002/anie.200804634.

Figure 1 shows a schematic illustration of our strategy for generating branched Au nanostructures. The key component is a three-dimensional lattice of uniform magnetic Fe nanoparticles which spontaneously forms on the surface of a magnetic stirrer bar. To increase the solubility of AuCl in the solvent, we incorporated it into a complex with oleyamine (OLA).[13] When the [AuCl(OLA)] complex is introduced into the reaction system, it quickly diffuses into the void space among the Fe nanoparticles and reacts with elemental Fe through the galvanic replacement reaction [Eq. (1)]:

$$3\,Au^{+} + Fe \rightarrow 3\,Au + Fe^{3+} \quad (1)$$

The resultant Au atoms then start to nucleate and gradually fill the voids between Fe nanoparticles as the reaction proceeds. As shown in Equation (1), consumption of one Fe atom produce three Au atoms, so the volume of Au nanostructure inside each void is expected to expand much faster than the volume shrinkage associated with the Fe nanoparticles. This net expansion in volume is expected to push the Fe nanoparticles apart, weakening the magnetic attraction between the Fe nanoparticles. The magnetic moments of the Fe nanoparticles are also gradually reduced during the replacement reaction, as a result of Fe consumption,[14] causing the lattice of Fe nanoparticles to fall apart into the reaction solution, accompanied by the release of the formed Au multipods (branched structures with more than two arms). Samples of pure Au multipods could be obtained by selectively dissolving the remaining Fe nanoparticles with H_2SO_4, together with centrifugation.

Low-magnification TEM imaging of the as-prepared Au multipods (Figure 2a) indicated that there were essentially no Fe nanoparticles remaining in the sample. TEM imaging at a higher magnification (Figure 2b) clearly indicated that the majority of the Au multipods formed with a complex branched structure. The branches were 8–10 nm in thickness, whereas the overall sizes of the multipods varied from 30 to 100 nm, in accordance with their diverse geometries. High-resolution TEM imaging (Figure 2c and Figure S1 in the Supporting Information) of a single Au multipod indicated that it contained crystal defects and lattice distortions. All the peaks of an X-ray diffraction (XRD) pattern taken from the same sample of Au multipods (Figure 2d) could be indexed to pure fcc Au (JCPDS 04-0784).

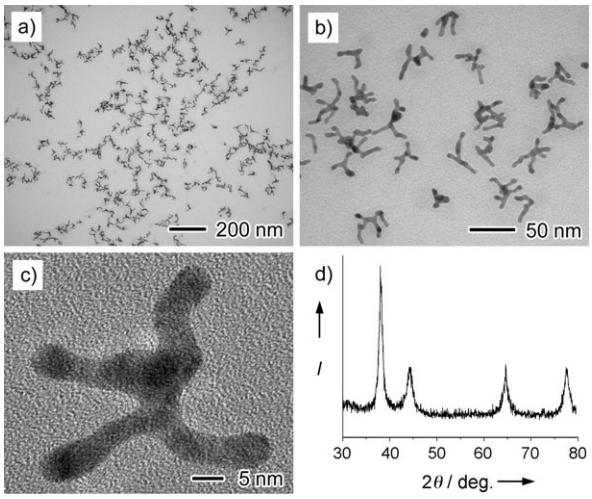

Figure 2. a, b) TEM images of the as-prepared Au multipods at different magnification; c) high-resolution TEM image of a typical Au multipod (see Figure S1 in the Supporting Information for details); and d) XRD pattern taken from the Au multipods.

To experimentally decipher the mechanism for formation of the Au multipods, we used TEM to check the intermediate products obtained at different stages of a typical synthesis. Before the addition of the [AuCl(OLA)] complex, the Fe nanoparticles mainly existed as black aggregates on the magnetic stirrer bar (Figure 3a, inset). A TEM image of Fe nanoparticles that were removed from the stirrer bar by ultrasonic treatment and subsequently drop-cast onto a copper grid (Figure 3a) shows the nanoparticles to be approximately spherical in shape, with a uniform diameter of (15 ± 1.6) nm. The actual size of these Fe nanoparticles should be slightly smaller than the size measured from the TEM image, because the surfaces of these nanoparticles were inevitably oxidized during TEM sample preparation. After adding [AuCl(OLA)] to the solution and stirring for 2 minutes, some black solid started to disassemble from the stirrer bar and diffuse into the solution. The initial disassembled material was mainly made up of small chunks (Figure S2 in the Supporting Information), and each chunk was composed of Fe nanoparticles and Au multipods in a rather compact structure (Figure 3b). The Au multipods were evidently formed in the void space among Fe nanoparticles, suggesting that the Fe nanoparticles served not only as a reducing agent, but also as a template for the formation of Au

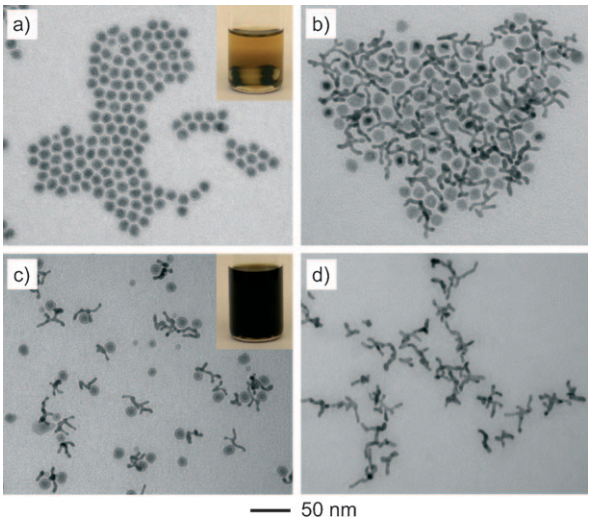

Figure 3. TEM images of samples obtained at different stages of the replacement reaction: a) Fe nanoparticles before the reaction, which were released from the stirrer bar by sonication; b) black solid initially disassembled from the stirrer bar, after adding [AuCl(OLA)] and stirring for 2 min; c) completely disassembled Fe nanoparticles and Au multipods, after continuous stirring for 20 min; and d) Au multipods, purified by washing the sample with 1 M H_2SO_4/C_2H_5OH solution to selectively dissolve the remaining Fe nanoparticles.

multipods. After stirring the solution for a further 20 minutes, more black chunks were separated from the stirrer bar and most of them further dissembled into discrete Fe nanoparticles, resulting in the formation of isolated Au multipods (Figure 3c). Concurrently, the color of the solution gradually changed into black (Figure 3c, inset), as a result of the complete disassembly of Fe nanoparticles. The TEM image of the final product (Figure 3d), after washing with 1M H_2SO_4/C_2H_5OH, showed that the remaining Fe nanoparticles had been completely removed, leaving behind Au multipods with essentially the same branched morphology. These experimental observations agree well with the schematic illustration shown in Figure 1.

Both the aggregate state of Fe nanoparticles and the oxidation state of Au played critical roles in the formation of branched Au multipods. In the synthesis of Fe nanoparticles, some of them (approximately 10% by weight) remained in the solution and did not aggregate on the stirrer bar (Figure S3 in the Supporting Information), presumably owing to their smaller sizes. When these non-aggregate Fe nanoparticles were used as a reactant and mixed with the [AuCl(OLA)] complex under the same condition as used in the synthesis of Au multipods, only Au nanoparticles were obtained and no branched structures were detected (Figure S4 in the Supporting Information). This result confirmed that only the Fe nanoparticles in an aggregated state could act as a template to generate Au multipods. Otherwise, Au nanoparticles were produced by direct galvanic replacement of suspended Fe nanoparticles with the Au^+ ions in the solution. In another experiment, when AuCl was replaced with the same molar amount of $HAuCl_4$ to react with a three-dimensional lattice of Fe nanoparticles, some small Au nanoparticles and L-shaped bipods were obtained (Figure S4 in the Supporting Information). In this case, the oxidization of one Fe atom to Fe^{3+} only generated one Au atom so that the net volume expansion for the system was negligible. As a result, the Au nanostructures that formed in the voids could not effectively push and loosen the aggregation of the surrounding Fe nanoparticles and grow into a multipod shape. The L-shaped bipods might be formed through the galvanic replacement reaction of Au^{3+} and Fe along the surface of some active Fe nanoparticles. Except for the aggregation state of Fe nanoparticles and the oxidation state of Au ions, other variables such as solvent did not have a significant influence on the formation of Au multipods. Au multipods were readily obtained using either tetrahydrofuran or dichloromethane as the solvent (Figure S5 in the Supporting Information).

Because the as-synthesized Au multipods contained defects and lattice distortions, they were found to show different oxidative etching behaviors in various acids. Figures 4a and b show TEM images of Au multipods after they had been washed with 1M HNO_3/C_2H_5OH and 1M HCl/C_2H_5OH for 5 minutes, respectively. No apparent morphological change occurred when the multipods were washed by H_2SO_4 (Figure 3d) or HNO_3 (Figure 4a), thus indicating that these two acids could not be combined with oxygen (from air) to form etchants for the Au multipods. However, the Au multipods were etched by 1M HCl/C_2H_5OH to become

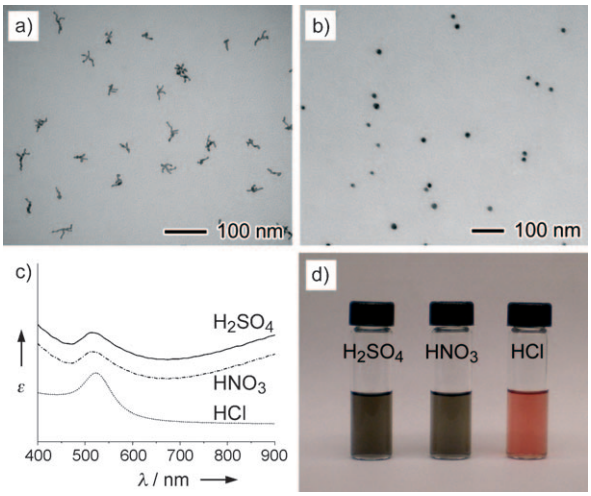

Figure 4. a, b) TEM images of the Au multipods after washing with 1M HNO_3/C_2H_5OH and 1M H_2SO_4/C_2H_5OH, respectively. c) Extinction spectra and photographs of Au multipods dispersed in hexane after washing with 1M ethanolic solutions of H_2SO_4, HNO_3, and HCl. Note that the spectra are vertically shifted for display purposes, so absolute peak height is not proportionate to the absorbance. d) Photograph showing color changes on washing a Au multipod dispersion in hexane with H_2SO_4, HNO_3, and HCl.

nanoparticles (Figure 4b). The same result was also obtained by replacing HCl with an equimolar mixture of HNO_3 and NaCl (1M solution in C_2H_5OH). The different etching behaviors of Au multipods in different acids can be attributed to the fact that Cl^- can act as a ligand to form complexes with Au ions (e.g., $[AuCl_2]^-$ or $[AuCl_4]^-$), whereas both NO_3^- and SO_4^{2-} ions have no such capacity. Previous studies have shown that multiply twinned metal nanostructures are susceptible to oxidative etching, owing to the high density of defects on the surface and resultant high reactivity. For oxidative etching to occur, a ligand is generally required to enhance the etching power of oxygen.[15] Since the Au multipods synthesized using the present method contained defects and lattice distortions, they are expected to exhibit higher reactivity than the single-crystalline Au nanostructures. High-resolution TEM imaging indicated that the Au nanoparticles left behind from HCl etching were single crystals (Figure S6 in the Supporting Information), confirming that the oxidative etching mainly attacked the defect zones on the Au multipods. The Au nanoparticles were spherical in shape and their average diameters were a little bigger than the sizes of the pods, suggesting that an Ostwald ripening process[16] might be involved during the oxidative etching process.

Figure 4c shows the extinction spectra taken from Au multipods dispersed in hexane after washing with different acids. The spectroscopic profile of the Au multipods washed with HNO_3 was similar to that of those washed with H_2SO_4, with a peak around 520 nm, ascribed to the transverse mode, and a broad peak in the near-infrared (NIR) region, resulting from the longitudinal mode of the rodlike arms of the multipods.[17] Multipods washed with HCl only gave rise to the peak at 520 nm, indicating the formation of spherical Au nanoparticles. The Vis/NIR spectra were consistent with

TEM observations of the corresponding samples. The morphological changes of Au multipods in different acids, coupled with the variations of their absorption spectra, could also be easily appreciated from their different colors (Figure 4d).

In summary, we have demonstrated a simple, template-directed method for generating Au multipods. The template wa a three-dimensional lattice, self-assembled in situ from magnetic Fe nanoparticles on a magnetic stirrer bar. When treated with [AuCl(OLA)], the void spaces among the Fe nanoparticles were gradually filled by the galvanic replacement reaction between Fe and Au^{+}. During this reaction, both the volume expansion associated with Au/Fe replacement and the consumption of Fe gradually weakened the attraction between the Fe nanoparticles. As a result, the lattice of Fe nanoparticles spontaneously fell apart to automatically release the Au multipods. The remaining Fe nanoparticles were readily removed by washing the samples with acids such as H_2SO_4 or HNO_3. Unlike previously reported star-shaped gold nanoparticles, these Au multipods were mainly composed of branched arms and showed a broad absorption peak in the NIR region. This interesting optical property suggests that these Au multipods might have potential use in applications such as NIR-based photothermal therapy, chemical sensing, and fabrication of flexible and conductive composite materials.

Experimental Section

The Fe nanoparticles were synthesized by thermal decomposition of $[Fe(CO)_5]$ in octadecene with OLA as a capping agent.[9b] The majority of the Fe nanoparticles (approximately 90% by weight) aggregated onto the magnetic stirrer bar used for the synthesis, which was transferred to a vial containing chloroform (3 mL, see the Supporting Information for details). In a typical synthesis of Au multipods, a stock solution of [AuCl(OLA)] complex (0.01M, 10 mL) was prepared by dissolving AuCl (0.0233 g, 0.1 mmol) in a mixture of chloroform (9.67 mL) and OLA (0.33 mL).[13] [AuCl(OLA)] solution (2 mL) was slowly added to the vial that contained the Fe nanoparticle aggregates on the stirrer bar. The reaction mixture was stirred (300 rpm) for 20 min. During this process, the Fe nanoparticles were gradually released from the stirrer bar and the chloroform solution became black. After dilution of the solution with an equal volume of acetone a mixture of Au multipods and suspended Fe nanoparticles was removed by centrifugation. The crude product was then dispersed in hexane (5 mL) and treated with of 1M ethanolic H_2SO_4 (three portions of 5 mL) to remove Fe nanoparticles. Pure Au multipods were collected following centrifugation and subsequently dispersed in hexane for further characterization.

Received: September 21, 2008
Published online: November 5, 2008

Keywords: electron microscopy · gold · iron · nanostructures · template synthesis

[1] Recent reviews: a) Y. Xia, Y. Xiong, B. Lim, S. E. Skrabalak, *Angew. Chem.* **2008**, DOI: 10.1002/ange.200802248; *Angew. Chem. Int. Ed.* **2008**, DOI: 10.1002/anie.200802248; b) A. R. Tao, S. Habas, P. Yang, *Small* **2008**, *4*, 310; c) Y. W. Jun, J. S. Choi, J. W. Cheon, *Angew. Chem.* **2006**, *118*, 3492; *Angew. Chem. Int. Ed.* **2006**, *45*, 3414; d) C. Burda, X. Chen, R. Narayanan, M. A. El-Sayed, *Chem. Rev.* **2005**, *105*, 1025.

[2] Recent reviews: a) M. Hu, J. Chen, Z. Y. Li, L. Au, G. V. Hartland, X. Li, M. Marquez, Y. Xia, *Chem. Soc. Rev.* **2006**, *35*, 1084; b) S. Eustis, M. A. El-Sayed, *Chem. Soc. Rev.* **2006**, *35*, 209; c) M. C. Daniel, D. Astruc, *Chem. Rev.* **2004**, *104*, 293; d) L. M. Liz-Marzán, *Mater. Today* **2004**, *7*, 26; e) M. A. El-Sayed, *Acc. Chem. Res.* **2001**, *34*, 257.

[3] C. J. Murphy, T. K. Sau, A. Gole, C. J. Orendorff, *MRS Bull.* **2005**, *30*, 349.

[4] a) C. H. Kuo, M. H. Huang, *Langmuir* **2005**, *21*, 2012; b) H. Y. Wu, M. Liu, M. H. Huang, *J. Phys. Chem. B* **2006**, *110*, 19291; c) X. Zou, E. Ying, S. Dong, *Nanotechnology* **2006**, *17*, 4758; d) J. Xie, J. Y. Lee, D. I. C. Wang, *Chem. Mater.* **2007**, *19*, 2823.

[5] a) E. Hao, R. C. Bailey, G. C. Schatz, J. T. Hupp, S. Li, *Nano Lett.* **2004**, *4*, 327; b) O. M. Bakr, B. H. Wunsch, F. Stellacci, *Chem. Mater.* **2006**, *18*, 3297.

[6] See, for example, a) L. Manna, D. J. Milliron, A. Meisel, E. C. Scher, A. P. Alivisatos, *Nat. Mater.* **2003**, *2*, 382; b) D. J. Milliron, S. M. Hughes, Y. Cui, L. Manna, J. Li, L. W. Wang, A. P. Alivisatos, *Nature* **2004**, *430*, 190; c) T. Mokari, E. Rothenberg, I. Popov, R. Costi, U. Banin, *Science* **2004**, *304*, 1787; d) Z. A. Peng, X. Peng, *J. Am. Chem. Soc.* **2002**, *124*, 3343.

[7] a) C. L. Nehl, H. Liao, J. H. Hafner, *Nano Lett.* **2006**, *6*, 683; b) M. Yamamoto, Y. Kashiwagi, T. Sakata, H. Mori, M. Nakamoto, *Chem. Mater.* **2005**, *17*, 5391; c) T. K. Sau, C. J. Murphy, *J. Am. Chem. Soc.* **2004**, *126*, 8648; d) S. Chen, Z. L. Wang, J. Ballato, S. H. Foulger, D. L. Carroll, *J. Am. Chem. Soc.* **2003**, *125*, 16186.

[8] a) J. C. Hulteen, C. R. Martin, *J. Mater. Chem.* **1997**, *7*, 1075; b) C. R. Martin, *Acc. Chem. Res.* **1995**, *28*, 61.

[9] a) F. Dumestre, B. Chaudret, C. Amiens, P. Renaud, P. Fejes, *Science* **2004**, *303*, 821; b) S. Peng, C. Wang, J. Xie, S. Sun, *J. Am. Chem. Soc.* **2006**, *128*, 10676; c) S. J. Park, S. Kim, S. Lee, Z. G. Khim, K. Char, T. Hyeon, *J. Am. Chem. Soc.* **2000**, *122*, 8581.

[10] L. Au, X. Lu, Y. Xia, *Adv. Mater.* **2008**, *20*, 2517.

[11] a) O. D. Velev, T. A. Jede, R. F. Lobo, A. M. Lenhoff, *Nature* **1997**, *389*, 447; b) B. T. Holland, C. F. Blanford, A. Stein, *Science* **1998**, *281*, 538; c) Y. Wang, A. S. Angelatos, F. Caruso, *Chem. Mater.* **2008**, *20*, 848.

[12] F. Li, Z. Y. Wang, A. Stein, *Angew. Chem.* **2007**, *119*, 1917; *Angew. Chem. Int. Ed.* **2007**, *46*, 1885.

[13] X. Lu, H. Y. Tuan, B. A. Korgel, Y. Xia, *Chem. Eur. J.* **2008**, *14*, 1584.

[14] D. L. Huber, *Small* **2005**, *1*, 482.

[15] a) B. Wiley, T. Herricks, Y. Sun, Y. Xia, *Nano Lett.* **2004**, *4*, 1733; b) Y. Xiong, J. Chen, B. Wiley, Y. Xia, *J. Am. Chem. Soc.* **2005**, *127*, 7332; c) N. Zettsu, J. M. McLellan, B. Wiley, Y. Yin, Z. Y. Li, Y. Xia, *Angew. Chem.* **2006**, *118*, 1310; *Angew. Chem. Int. Ed.* **2006**, *45*, 1288.

[16] a) Z. A. Peng, X. G. Peng, *J. Am. Chem. Soc.* **2001**, *123*, 1389; b) R. F. Li, Z. T. Luo, F. Papadimitrakopoulos, *J. Am. Chem. Soc.* **2006**, *128*, 6280.

[17] a) C. L. Nehl, J. H. Hafner, *J. Mater. Chem.* **2008**, *18*, 2415; b) S. Link, M. B. Mohamed, M. A. El-Sayed, *J. Phys. Chem. B* **1999**, *103*, 3073.

